Geochemistry exploration environment analysis of waters: the case of the basin of the Great Sebkha of Oran

N. Boualla, A. Benziane and K. Ait-Mokhtar

ABSTRACT

Water resources are economically and environmentally the most valuable for countries affected by aridity. This study is to identify the factors influencing the quality of the waters of the aquifer system of the Great Sebkha of Oran, one area that is already in a stress situation. The determination of the origin of the salinity of the waters was approached from an analysis of the chemical type. Water mineralization is mainly governed by the phenomena of dissolution and precipitation of minerals (calcite, dolomite, anhydrite, gypsum and halite).

Key words | correlation, ionic balance, physical-chemical parameters, saturation index

N. Boualla (corresponding author)
A. Benziane
Université des Sciences et de la Technologie d'Oran Mohamed Boudiaf, USTO-MB,
BP 1505, El M'naouer,
31000 Oran/Laboratoire LMST,
Algérie
E-mail: *nabila.boualla@univ-usto.dz*; *nibrasnabila@yahoo.fr*

K. Ait-Mokhtar
Université de La Rochelle,
LaSIE UMR CNRS 7356,
Avenue Michel Crépeau – 17042 La Rochelle cedex 1,
France

INTRODUCTION

Scarcity of water, pollution load, political issues and rising population have drawn great attention to the proper management of water resources such as groundwater in the 21st century (Benouara *et al.* 2016).

The basin of the Great Sebkha of Oran is characterized by endorheic drainage. In this agricultural space, the most widely used irrigation system is drip. Water supply is one of the determining factors in agricultural production, both in crop intensification and extension of irrigation. Water deficit linked to climate semi-aridity has forced farmers to resort to the use of underground water of poor quality which is not without consequences for land degradation.

Environmental data are strongly characterized by inherent variability, and only limited understanding of the environmental distribution of contaminants can be gained from chemical analysis (Machiwal & Jha 2015). The complex and highly variable geological and lithological scenarios combine the content of the major chemical components and dissolved CO_2, and will determine their healthy properties and uses. These factors create spatially different water types (i.e. hydrochemical facies) (Ciotoli & Guerra 2016).

Our study is based on the collection of samples of surface water and groundwater collected in pretty well-distributed points throughout the basin (Table 1 and Figure 1).

The results show that pumping-induced hydraulic gradient changes and artificial connection of aquifers by well screens can mix chemically distinct groundwater (Ayotte *et al.* 2011). Correlations between major elements highlight the main mechanisms involved in the evolution of the salinity of the water in the different horizons of the aquifer system and map the vulnerability of soils.

GEOLOGICAL AND HYDROGEOLOGICAL CONTEXT

The basin of the Great Sebkha of Oran is located in northwestern Algeria (Figure 2). It extends over an area of 1,890 km^2 of which 298 km^2 are occupied by the Sebkha. This salt lake is over 40 km long and 6 to 13 km wide.

Geological studies have highlighted a structure consisting of three estates: a native bedrock ante nappe Mesozoic forming the backbone of the massif to the schistosity of Murdjadjo, to the north; a complex of allochthonous units put in place in the Miocene forming the Tessala mountains to the south; and sedimentation post nappe Neogene and Quaternary, subsiding in the central area. The formations thus defined generally have lateral variations in thickness and facies (Figure 1).

doi: 10.2166/ws.2017.076

Table 1 | Network measurement and sampling

N°	Nature	Name	UTM		
			X	Y	Z
1	Drilling	Oued Tlélat OT2 Bis	720.654	3,933.795	107
2	Drilling	Oued Tlélat OT5	722.975	3,938.85	100
3	Drilling	Oued Tlélat OT7	719.975	3,939.495	90
4	Wells	TOUATI	696.875	3,938.55	92
5	Wells	Orangerie	696.7	3,939.95	112
6	Wells	BELHADRI Abdelkader	700.725	3,942.35	143
7	Source	Ain Beida	683.525	3,922.55	94
8	Drilling	Moulin Mokhtar el Oumda	695.975	3,920.87	113
9	Wells	CHEHEIDA Belgacem	697.25	3,923.05	109
10	Drilling	MOULAY Said	697.325	3,925.42	101
11	Wells	Kratsa	700.85	3,928.85	98
12	Drilling	Kratsa	701.47	3,928.457	99
13	Wells	DELLA-KRACHAI Boumediène	694.975	3,939	100
14	Drilling	BOUDINAR Ahmed	693.625	3,944.05	480
15	Drilling	Ain el Arba {Frères Aziz F1)	691.575	3,919.75	105
16	Oued	Oued el Ared	720.875	3,938.575	89
17	Wells	Bou Tlélis (Pépinière)	693.1	3,938.35	91
18	Wells	ABDELLI Said N°2	706.875	3,943.56	117
19	Wells		707.34	3,943.275	110
20	Wells	HAMMADI Mohammed	707.475	3,943.175	104
21	Wells	Ex-Ferme Saint Pierre	707.8	3,943.175	108
22	Wells	CHETTIR Noureddin N°1 1	706.57	3,942	91
23	Wells	SENOUCI Ali N°1	708.775	3,942.75	88
24	Wells	MAHMOUDI Mohamed	705.87	3,942.425	98
25	Wells	CHIKHI	688.05	3,936.2	85
26	Wells	KARAMA Houari (Domaine Mimoun)	685.45	3,935.75	86
27	Drilling	DHEIMI Moulay	695,150	3,938.92	92
28	Wells	ABBOU Kouider	692.675	3,938.05	86
29	Wells	MOSTAGHALM (Rios)	693.2	3,938	89
30	Drilling	M'lèta N°2	718.895	3,934.508	96
31	Wells		720.675	3,928.1	156
32	Drilling	Misserghin F9	701.047	3,941.592	122
33	Drilling	S sec 2	695.368	3,939.124	105
34	Drilling	S sec 3	698.794	3,940.176	99.8
35	Drilling	S, Sidi Salem	704.64	3,943.724	128
36	Drilling	S, de Misserghin syndic,	704.807	3,943.433	118
37	Drilling	S, Ban Lartigue 2	723.729	3,933.812	106
38	Drilling	SE7A	718.032	3,928.71	108.8

(*continued*)

Table 1 | continued

N°	Nature	Name	UTM X	UTM Y	UTM Z
39	Drilling	S4A	717.921	3,928.723	107.3
40	Drilling	S, Douar Saida	702.647	3,919.456	134
41	Drilling	S, Hammam bou hadjar	687.452	3,918.822	140
42	Drilling	Ain Arbaa	691.526	3,919.41	109
43	Wells	Flaga Abdelkader	721.873	3,929.194	130
44	Drilling	Tafaraoui N°2	723.591	3,934.105	120
45	Drilling	S, Misserghin	703.52	3,943.157	115
46	Wells	Berial F4	697.836	3,940.1	104
47	Wells	Station de service Tamazourah	712.95	3,920.75	181.5
48	Wells		717.685	3,929.55	98
49	Wells		704.875	3,944.5	140
50	Wells	Station Tamazourah 2	712.962	3,920.775	181.5
51	Oued	Oued Rassoul	706.457	3,918.5	163
52	Oued	Oued Haimeur	701.613	3,916.599	165
53	Oued	Oued Tafaraoui	723.551	3,929.71	156
54	Oued	Oued Tamazourah	713.105	3,920.378	188
55	Oued	Oued Besbas (Oued Tleta)	697.614	3,917.024	153

The aquifer system is made by stacking, depending on the location, two to three layers of aquifers: the Miocene limestone, sandstone and sandy Pliocene and Quaternary alluvium.

MATERIALS AND METHODS

For the purposes of the study of the geochemical characterization of the aquifer system, we have selected 55 water points pretty well distributed all around the lake of the Great Sebkha of Oran. This network is restricted compared with that constituted originally (93 points) for various reasons, namely the drying up of the oued and some sources, and the poor state or the abandonment of some wells. More than 95% of the network permanently retained and listed consists of wells for irrigation of crops and also for domestic use (Table 1 and Figure 1).

The collection of water samples was held during low flow, 4–20 July 2011. These samples were analyzed in the laboratories of applied geology at the University of Sciences and Technology of Oran and Centre University of Tlemcen according to methods described in Table 2.

RESULTS AND DISCUSSION

Critical analysis of the results

The results were verified by calculation of the ion balance (Table 3). In theory, a chemical analysis is considered as reliable only if the balance is less than or equal to 5%. The reliability of the data of the analysis has also been verified by simple linear regression between the sum of cations and anions, on the one hand, and between the electrical conductivity and the amount of ions, on the other hand. The balance calculated for all of the samples is surplus to 87% in anions. This surplus could, in the case of waters relatively loaded with dissolved salts, be explained by the existence other, unscanned cations, or erroneous results.

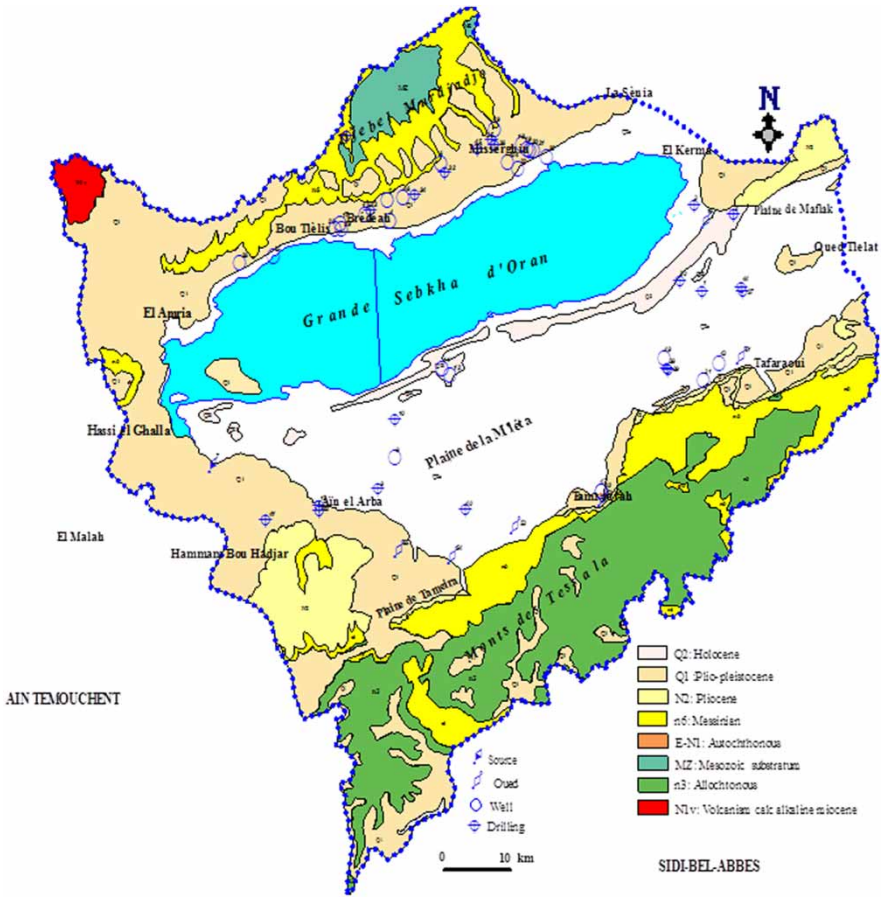

Figure 1 | Geological map (Benziane 2013) and location of sampling points.

Changes in factors such as groundwater pH, ion exchange, and ion complexation, may be initiated or enhanced by agricultural inputs and irrigation, which also can substantially change the major-ion composition of the groundwater (Dubrovsky *et al.* 1993; Fujii & Swain 1995; Szabo *et al.* 1997; Seiler *et al.* 2003; Böhlke *et al.* 2007).

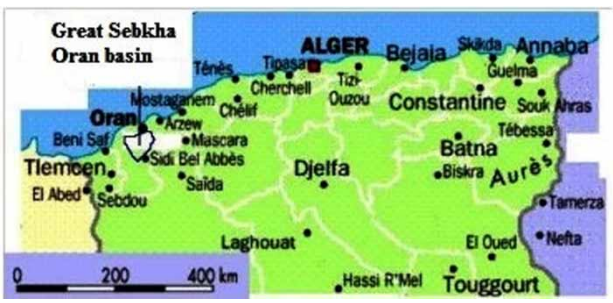

Figure 2 | Location of the study area (Benziane 2013).

The determination of the monovalent cations Na^+ and K^+ by the method of electrolytes is likely doubtful. Indeed, these results compared with those of previous analyses by

Table 2 | Analytical methods and apparatus used

Parameter	Method and apparatus
pH	Analyzer multi-parameter portable Mark Hanna instrument model HI 9811
Electrical conductivity	
HCO_3^-	Volumetric
Mg^{2+}	
Cl^-	
Ca^{2+}	
SO_4^{2-}	Spectrometry, spectrometer Optizen 2120 UV
Na^+	Ionogram Easy lyte Na/K/Cl, 800 ml, MEDICA 001384-001 R2 Analyzer, 12160/12014-05
K^+	

Table 3 | Measurements and chemical analysis results

N°	T (°C)	pH	σ (µS/cm)	Ca^{+2} (mg/l)	Mg^{+2}	HCO_3^-	Na^+	K^+	Cl^-	SO_4^-
1	34	6.7	3,450	380	764	3,630	310.5	5.07	2,157.7	307.7
2	22	6.8	4,060	200	644	1,605	356.5	5.85	1,727.6	311.6
3	33.5	6.3	6,880	200	836	1,901	715.3	7.02	2,485	310
4	26	6.7	7,250	220	3,265	11,359	623.3	6.63	7,976	299.4
5	27	7	5,170	240	536	1,417	602.6	5.85	2,094.5	300.6
6	24	7.2	3,150	248	2,037	7,776	333.5	2.34	4,775	294.2
7	24.5	7.4	6,080	180	692	12,084	4,687.4	31.59	5,994.5	297.2
8	30	6.8	7,650	260	956	3,509	894.7	3.12	2,995	320.2
9	22	6.6	15,820	288	2,396	1,356	818.8	36.27	7,810	368.7
10	24	6.9	10,300	192	1,580	8,162	2,267.8	21.84	4,960	345.4
11	22.5	6.7	11,370	176	2,036	9,528	2,037.8	6.24	5,551	400.4
12	26	6.9	4,920	208	548	2,595	1,106.3	4.29	2,123.5	322.1
13	25.5	6.9	7,810	340	1,040	4,242	871.7	8.19	2,378.5	302.1
14	27	6.9	1,450	156	368	816	184	3.51	1,136	299.3
15	/	6.9	3,500	280	896	3,191	623.3	13.65	3,094.5	295.7
16	27	7.2	6,770	180	1,472	5,732	756.7	7.02	4,307.5	319.1
17	26	6.3	12,850	460	1,388	3,086	1,642.2	12.48	5,970	315.2
18	24.5	6.4	6,760	680	1,844	8,414	1,067.2	13.26	5,669	312.2
19	24	6.5	6,920	380	2,444	11,000	1,117.8	13.26	6,684	320.7
20	23	6.6	6,260	440	2,516	11,194	1,016.6	14.82	6,417.5	310.2
21	25	6.4	6,240	520	2,516	10,904	1,025.8	15.99	6,607.5	308.8
22	21.5	6.6	7,550	600	2,504	12,060	1,179.9	3.12	6,617.5	315.4
23	22	6.9	2,300	320	344	421	384.1	0.858	1,775	297.2
24	23.5	6.6	6,360	600	800	3,053	1,018.9	10.53	3,288.5	309
25	32	6.8	6,790	300	1,040	3,090	535.9	8.58	2,685	315.5
26	21	6.9	13,360	304	1,892	4,356	1,752.6	24.18	5,970	307.1
27	27.5	6.8	8,140	236	1,000	2,036	848.7	8.19	3,372.5	313.7
28	26	6.4	11,330	460	1,532	6,193	1,212.1	8.97	5,408	304.4
29	26	6.5	8,760	348	1,244	4,481	800.4	8.19	3,662.5	328.7
30	27	7.5	8,130	192	1,652	7,789	1,166.1	3.51	5,272	321.9
31	31	6.8	4,460	184	1,532	6,521	713	1.95	4,952.5	307.8
32	27	7.3	1,240	160	1,196	5,000	167.9	3.51	2,994	294.1
33	/	6.9	5,310	316	1,364	3,462	181.7	2.73	2,965.5	301.5
34	/	7.5	950	420	812	3,520	177.1	2.73	2,207	295.7
35	/	7.5	730	200	596	1,634	158.7	1.95	1,100.5	302.9
36	21	7.1	3,300	200	668	2,226	370.3	9.75	1,584.5	300.8
37	40	6.9	4,350	340	1,124	5,595	372.6	6.24	3,065	318.8
38	/	7.2	3,020	400	500	2,095	618.7	3.12	1,775	299.4
39	29.5	6.9	3,610	460	4,125	14,330	342.7	3.51	9,100	308.1

(*continued*)

Table 3 | continued

N°	T (°C)	pH	σ (µS/cm)	Ca^{+2} (mg/l)	Mg^{+2}	HCO_3^-	Na^+	K^+	Cl^-	SO_4^-
40	27	7.6	1,060	120	465	450	230	2.34	1,597.5	296.5
41	24.5	5.1	9,350	420	644	2,541	1,345.5	42.51	3,324	299.4
42	28.5	6.8	5,020	360	725	1,534	483	8.58	2,307.5	from 297.5
43	25	6.9	6,040	380	656	2,246	979.8	3.9	2,591.5	311.1
44	36	6.5	4,070	460	500	2,062	158.7	3.12	1,065	312.7
45	/	7.4	720	184	212	1,616	1,000.5	11.7	1,455.5	296.1
46	26	7.1	8,240	236	740	3,288	1,451.3	2.34	3,769	313.1
47	25	6.8	4,680	180	740	470	692.3	6.63	3,017.5	323
48	24.5	6.9	7,850	220	855	1,566	733.7	5.85	2,769	305.7
49	21	7.4	1,030	216	1,415	941	124.2	1.95	3,550	297.6
50	27.5	6.9	4,830	460	4,525	19,962	708.4	7.8	8,907.5	313.6
51	/	6.5	5,000	360	300	2,038	805	5.46	1,520	343.6
52	/	6.7	8,800	400	432	3,848	1,734.2	8.97	3,775	367.7
53	/	7.1	4,630	160	408	1,495	630.2	3.12	1,420	342.3
54	/	7.3	3,410	80	1,420	4,433	437	4.29	2,775	329.2
55	/	7.3	5,710	240	480	2,214	929.2	5.85	2,100	325

the technique of atomic absorption on the same points of water are completely different, calling into question the method practiced in the laboratory of the CHU of Tlemcen.

Dissolution and electrical conductivity of materials

The electrical conductivity of a complex saline solution is the sum of the conductivities attributed to each of the ions it contains (Schoeller 1962). Measurements of electrical conductivity, operated *in situ*, reflect a concentration of salts dissolved in the different horizons of the aquifer system in the study area. The recorded values show sizeable variations, ranging from 720 to 15,820 µS/cm at points 45 and 9 (Table 3). These values, denoting the upstream to downstream growth, increase in measure as we approach the Sebkha Lake. This variation is certainly linked to the lithological nature of the aquifer and the depth of the deposit of water. The waters of the limestone formations, circulating in karst aquifer networks, have low values. High values are recorded at water points serving alluvial levels, characterized by many lateral passages and vertical facies (Figure 3). This is, indeed, a continental sedimentation detrital, heterogeneous from a size point-of-view. In general, the permeability in these environments is directly related to the grain size of the sediments. The more the granulometry is thin, the more the flows are slow and the mineral matrix–water contact time is long, which translates into a high concentration of mineralization.

Overall, these conductivity values are, in the majority, superior to the limits of the fixed potability standards in 2011 (180–1,000 µs/cm for WHO; ≤2,800 µS/cm for Algeria).

The dominant chemical facies are chloride–sodium, and chlorinated and sulfated forms of calcium and magnesium (Figure 4).

Figure 5 establishes the relationship between electrical conductivity and the anions. Overall, sulfate concentration increases, from the outset, and then stabilizes, which is accounted for by the blocking of these ions by organic reduction. As chlorides, they grow with the increase of conductivity, which translates into the relative enrichment of the waters in chlorides and the precipitation of carbonate minerals.

Relationship of Na^+ vs Cl^-

Several types of reactions between groundwater and rocks can be identified using traces of correlation with chlorine

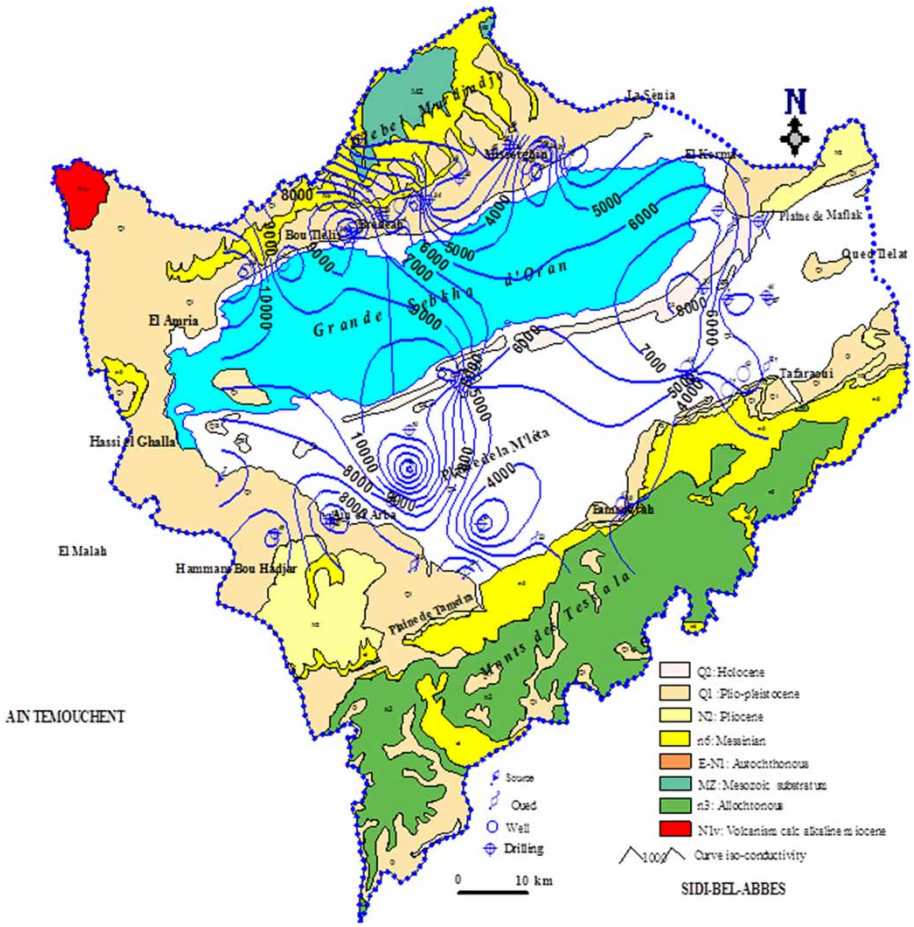

Figure 3 | Map showing curves of iso-values of electrical conductivity (μS/cm).

(Nordstrom *et al.* 1989). The latter is an item stored, not participating in water–rock interactions; He characterised the origin of the salinity of the water and is a mixture tracer (Fidelibus & Tulipano 1996). The origin of this element is linked primarily to the dissolution of salt formations and evaporation in closed environments (endorheic systems). In natural waters, the presence of both Na and Cl is attributed to the dissolution of halite that is found in the Triassic formations. Levels of Na^+ and Cl^- should be balanced. However the determination of the cation Na^+ obtained by the method of electrolytes gives a value deficit compared with the anion Cl^-. The ion Na^+ measured differently by the method of atomic absorption that seems to give more reliable values is taken into account in the delimitation of the right of the correlation (Benziane 2013). The relationship between these two ions is characterized by a strong correlation coefficient (Figure 6). This relationship shows that all the points are more or less aligned on the right equal to 1 indicating that these two elements have, in the majority of cases, the same origin. Overall, the reported Na^+/Cl^- is less than 1, indicating that the process of dissolution of alluvium salts (especially halite) is responsible for sodium content. However, the chlorides such as sodium may, exceptionally, have other origins (natural or anthropogenic). The deficit in Na which is from the phenomenon of inverse ion exchange between the water and the aquifer translates to an adsorption of Na^+ and a release of Ca^{++}. This can be explained by the deposition of salts under semi-arid to arid climatic conditions (low rainfall and high temperatures) or by the leaching of the marl land by rainwater. Understanding water storage changes in the basin and the related impacts of climate variability is an essential step in managing its water resources (Awange *et al.* 2014).

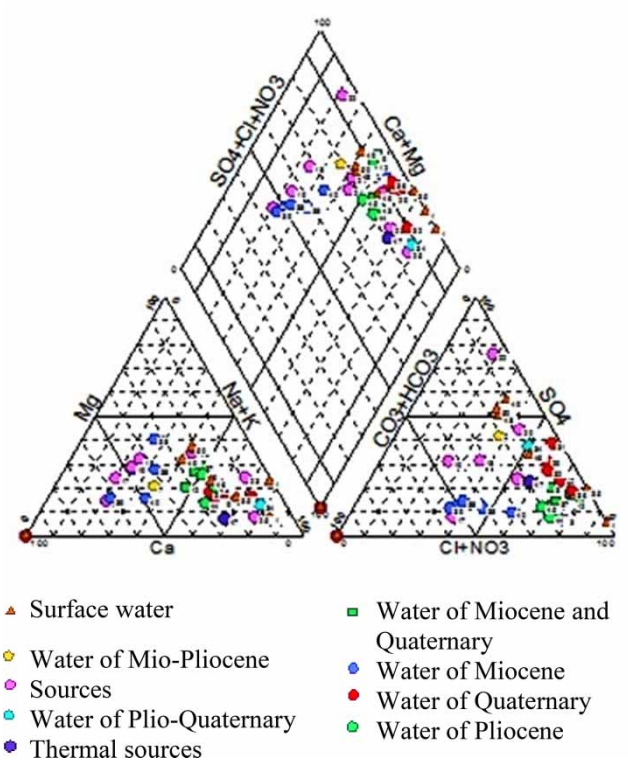

Figure 4 | Piper diagram (Benziane 2013).

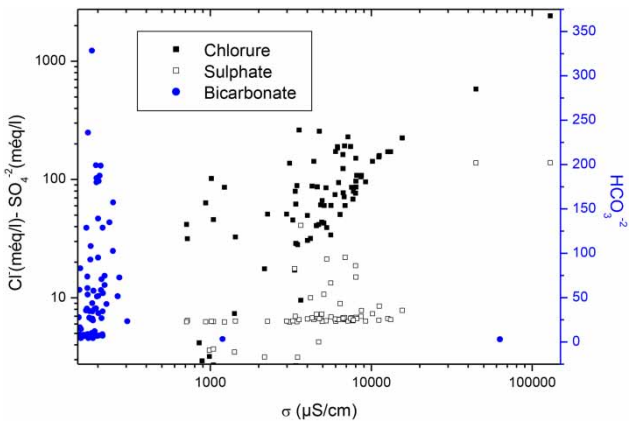

Figure 5 | Relationship of SO_4^{2-}, ^{-}Cl, and HCO_3^- versus conductivity.

Relationship of SO_4^- vs Cl^-

The geochemical control of sulfate is the most complex to interpret. The delimitation of the right of the theoretical evolution of solutions is problematic since the Cl^- and SO_4^- are not simultaneously at their maximum dilution rate. One can think in this case of a sulfate reduction to the level of sediment, confirmed in the area by evaporitic formations. This phenomenon would explain the huge annual consumption of the element sulfate accompanied by production of bicarbonate according to the general equation:

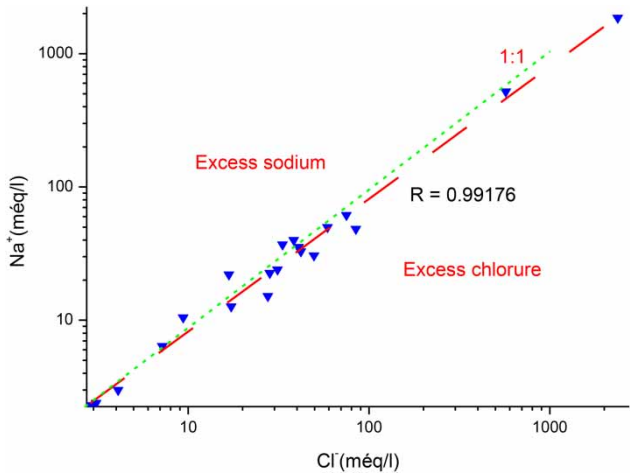

Figure 6 | Relationship of Na^+ versus Cl^-.

$$2Fe_2O + 15CH_2O + 8\,SO_4^- + H_2CO_3 \rightarrow 4FeS_2 + 16HCO_3^- + 8\,H_2O \quad (1)$$

where Fe_2O_3 is a red clay, residue of the dissolution of limestone, with depletion of SiO_2 and in Fe_2O_3 enrichment.

The relationship between chloride and sulfate shows a dispersion of points indicating a change of the two elements having a salt origin, common gypsiferous (Figure 7). The predominance of sulfates over chlorides or vice versa depends

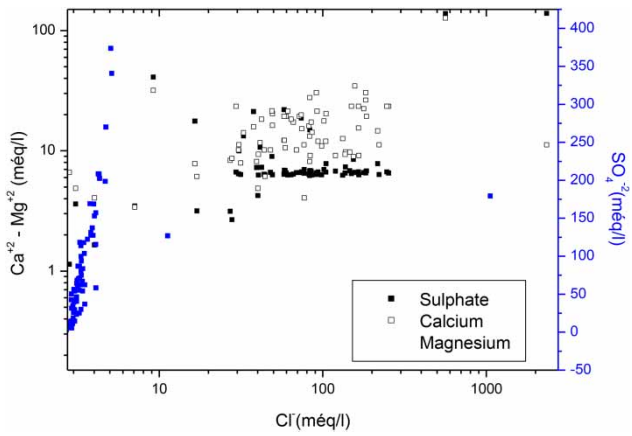

Figure 7 | Relationship of SO_4^{-2}, Mg^{+2}, and Ca^{+2} versus Cl^-.

essentially on the state of the minerals that generate these ions in water (equilibrium, oversaturated, undersaturated). The importance of the excess of one or the other element determines the dominance of the facies of that element over the other.

The levels of chlorides present values more important than sulfates, due to the special characteristics of that element. The chloride facies does not fit into the phenomena of chemical precipitation, was not adsorbed by the geological formations and is very mobile. The atmospheric origin assumes that sulfates and chlorides evolve together and in a similar way. An increase in chloride should be accompanied by that of sulfates. However, in the majority of our samples, this evolution is not highlighted. This concentration difference between chloride and sulfate does not seem to depend essentially on the nature of the land. Sulfate would mainly come from the dissolution of gypsum, widely represented in the basin, and secondary phenomena of oxidation–reduction of mineral and organic matter.

The graphical representation shows that the points have a reported (Cl^-/SO_4^-) greater than 1, indicating a dominance of the chloride ions over sulfate. This difference can be explained by the solubility of material washed away during the rainy episodes; halite is more soluble than gypsum.

In the plains from the edge of the lake, the origin of sulfate can come from the land application of fertilizers in intensive agriculture.

Origin of calcium

The calcium originates from carbonate minerals and gypsum. The determination of the origin of each Ca^{++} concentration is needed to understand the mechanisms of the affinity of the groundwater. Calcium release by the dissolution of the gypseous rocks as well as following the attack of rock carbonate by carbonic acid from the water–carbon dioxide reaction. Figure 8 represents the calcium bicarbonate versus sulfate relationship. The graph shows that the origin of the calcium is rather carbonate than evaporitic; the reported SO_4^-/HCO_3^- is always less than 1.

The relationship between the ions Ca^{++} and HCO_3^- is characteristic of the course of the groundwater. The low value of the Ca^{++}/HCO_3^- ratio (between 0.05 and 10)

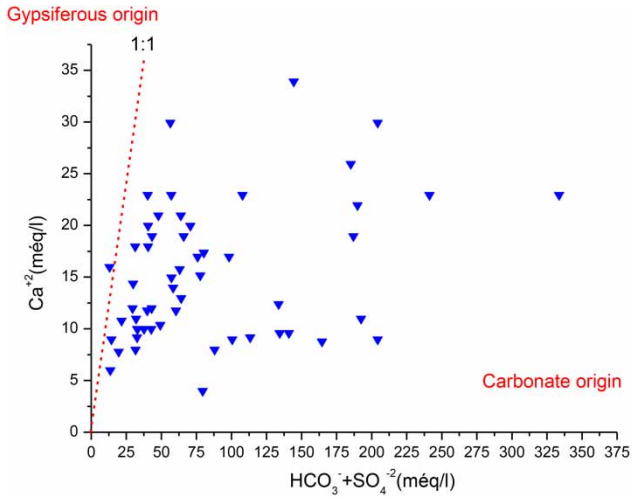

Figure 8 | Determination of the origin of calcium.

translated to the depletion of water in Ca^{++} causing an increase in the content of HCO_3^-. High concentration of HCO_3 can also be attributed to the CO_2 present in the soil. This CO_2 can also result from the water–rock interaction as is confirmed by the reported HCO_3^-/Σ anions (0.01–0.1) (Kortatsi *et al.* 2008).

Oxidation of organic matter by microbes generates CO_2, which then combines with water to form carbonic acid and dissociates to H and HCO_3 ions (Satyanarayanan *et al.* 2016).

$$CH_2O + O_2 \rightarrow CO_2 + H_2O \rightarrow H_2CO_3 \rightarrow H + HCO_3 \quad (2)$$

Low concentrations of Ca^{++} are due to the precipitation of carbonate of calcium in the summer. Taking into account the correlation between calcium and magnesium, an exchange of base is likely between these two elements (Brinis *et al.* 2004). The waters are more magnesian than calcium. The study of the reported Ca^{++}/Mg^{++} waters of this region advocated the dissolution of calcite and dolomite present in the Miocene aquifer. If the reported $Ca^{++}/Mg^{++} \leq 1$, the dissolution of dolomite should occur; a higher ratio (>1) is indicative of a contribution of more calcite (Mayo & Loucks 1995).

The reported Ca^{++}/SO_4^- (between 0.007 and 1.72) indicates that these two ions are at the origin of the dissolution of the gypseous and dolomitic formations. The study of the reported Ca^{++}/Mg^{++} of the waters of this region advocated

the dissolution of this dolomite at the level of the Miocene aquifer.

Mineral saturation indices

Using saturation index and activity diagrams, it is possible to predict the mineralogical reaction from groundwater data without collecting samples of the solid phase and mineralogical analysis (Deutsch 1997). Figure 9 shows that from the beginning of the concentration, the solutions are saturated to supersaturated in calcite and aragonite, overall saturated to balanced compared with dolomite and undersaturated with respect to anhydrite, gypsum and halite, which means that evaporate mineral phases are undersaturated and therefore favorable to dissolution along the path of groundwater flow.

The calculation of the minerals in the water saturation index shows that only carbonate minerals tend to precipitate, mostly in the form of dolomite (Figure 10).

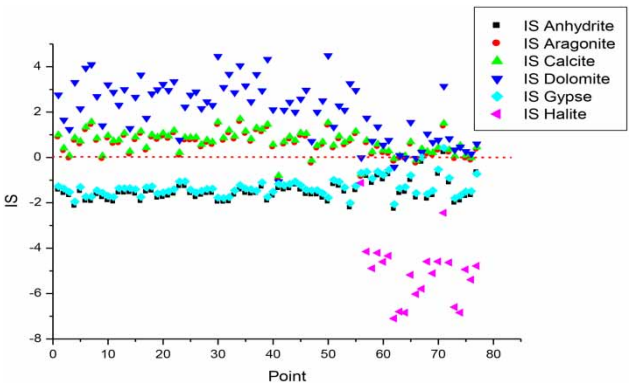

Figure 9 | Variation of mineral saturation index.

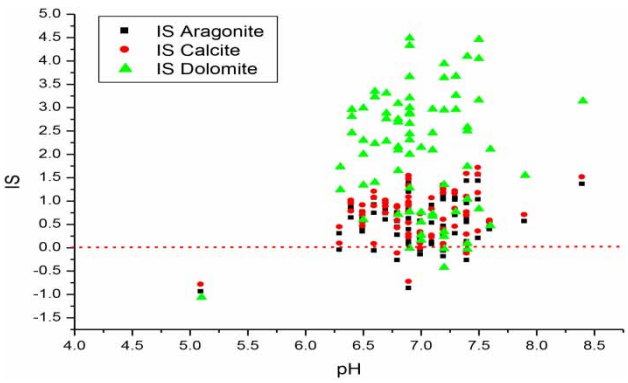

Figure 10 | Evolution of indices of saturation and pH.

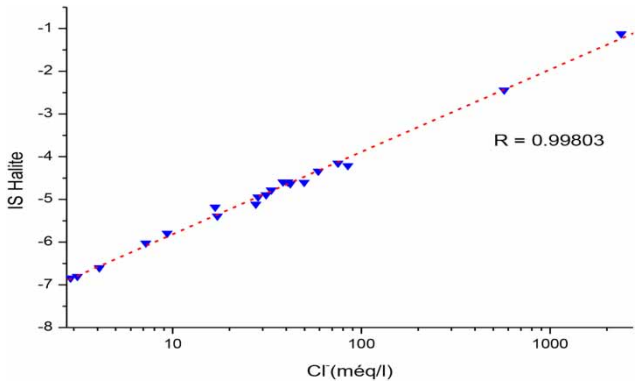

Figure 11 | IS halite–Cl concentration relationship.

Evaporates are always in the state of undersaturation, resulting in their rapid dissolution and allowing the ions Na^+, Cl^- and SO_4^- to stand in water with high concentrations. In the basin of the Great Sebkha of Oran, the main minerals constituting evaporates are gypsum, anhydrite, and halite.

For the study of calco-carbonic equilibrium, the graph of Figure 11 shows that indices of saturation of carbonate minerals have mean values of the order of 0.80 for calcite, 0.65 for aragonite and 1.49 for dolomite. These indices are mostly positive for calcite and aragonite, which involves precipitation processes. Only point 41 is marked by the dissolution of calcite. This last is a fast reaction and water can reach saturation through the unsaturated zone (Appelo & Postma 2005). The dissolution of the dolomite is slower than that of calcite (on the order of a few months). Note that they tend to become positive in the vicinity of a slightly alkaline pH (Figure 10).

The average values calculated for the index of saturation of the anhydrite and gypsum are respectively of the order −1.92 and −1.71. All samples are undersaturated in evaporites. The dissolution of gypsum promotes an increase in the concentration of calcium and thereby the reported Ca^{++}/Mg^{++}. Beyond 0.5, it causes the phenomenon of de-dolomitization, which seems to mark the water chemistry at points 23, 51 and 52 (Ammary 2007).

Halite is distinguished by its strong dissolution compared to that of gypsum and anhydrite. Figure 11 shows that the original brine binds a solution probably supersaturated in halite and the saturation index increases with the

concentration of chloride or halite-rich evaporites. Some processes are responsible for the losses of a quantity of sodium.

CONCLUSION

The geochemical study of the Water Company confirms mineralization is variable in relation to the lithological nature of the slopes and aquifers in the basin of the Great Sebkha of Oran. Generally, the salinity of the water increases upstream to downstream in the direction of the Sebkha. The alluvial aquifer waters distinguish themselves particularly compared with the other aquifers of the system by their relatively high concentration in dissolved salts (15,820 μS/cm at point 22). The exploitation of the results of analyses and their representation on appropriate diagrams highlight two dominant chemical facies: chloride-sodium, and calcium and magnesium chloride and sulfate. These waters, of poor quality, are unfit for domestic consumption. They are often used on sites for irrigation of parcels of land.

The origin of this natural salinity is attributed to the slopes of the basin, particularly leaching at Tessala where outcroppings of gypsiferous marls and salt occupy large spaces. The groundwater contained in the alluvial formations is, moreover, subject to exchanges with the atmosphere (evaporation and evapotranspiration) that tend in a closed space to concentrate more salts dissolved in the water. This degradation of the environment is often supported by anthropic action, also in crop intensification and extension of irrigation into the drinking water supply. Intensive and prolonged pumping is the source of intrusions, in the Miocene aquifer limestone of the Murdjadjo, of bodies of brackish water from the overlying alluvial medium. Geochemical evaluation has been instrumental in describing these problems (Edmunds 2009).

Finally the Sebkha, due to its altitude, its position and its role as an evaporating machine, would be at the origin of the salinity of the waters of the basin. This area requires special attention, as non-persistent pollutants may influence water quality (Vidal Montes *et al.* 2016). Often, when quality is not within the required standards and it is not used adequately, water can be a determining factor in baking for obtaining the desired dough and final product characteristics (Sinani *et al.* 2014).

REFERENCES

Ammary, B. 2007 *Étude géochimique et isotopique des principaux aquifères du bassin Crétacé d'Errachidia et de la plaine de Tafilalet*. Thèse de doctorat, Université Mohammed V – Agdal, Morocco.

Appelo, C. A. J. & Postma, D. 2005 *Geochemistry, Groundwater and Pollution*, 2nd edn. Balkema Publishers, Leiden, The Netherlands.

Awange, J. L., Forootan, E., Kuhn, M., Kusche, J. & Heck, B. 2014 Water storage changes and climate variability within the Nile Basin between 2002 and 2011. *Advances in Water Resources* **73**, 1–15.

Ayotte, J. D., Szabo, Z., Focazio, M. J. & Eberts, S. M. 2011 Effects of human-induced alteration of groundwater flow on concentrations of naturally-occurring trace elements at water-supply wells. *Appl. Geochemistry* **26**, 747–762.

Benouara, N., Laraba, A. & Hachemi Rachedi, L. 2016 Assessment of groundwater quality in the Seraidi region (north-east of Algeria) using NSF-WQI. *Water Science and Technology: Water Supply* **16** (4), 1132–1137.

Benziane, A. 2013 Le système aquifère de la Grande Sebkha d'Oran: considérations géologiques et hydrogéologiques. *Bulletin de l'Institut Scientifique, Rabat, Section Sciences de la Terre* **35**, 77–92.

Böhlke, J. K., Verstraeten, I. M. & Kraemer, T. F. 2007 Effects of surface-water irrigation on sources, fluxes, and residence times of water, nitrate, and uranium in an alluvial aquifer. *Appl. Geochem.* **22**, 152–174.

Brinis, N., Djabri, L. & Kardache, R. 2004 La salinité des eaux souterraines de la région Est de la plaine d'El-Outaya, Biskra, Algérie. In: *Colloque International Terre et Eau*, CIST, Terre–Eau, Département de géologie, Faculté des sciences de la terre, Université Badji Mokhtar, Annaba, Algeria, pp. 273–276.

Ciotoli, G. & Guerra, M. 2016 Distribution and physico-chemical data of Italian bottled natural mineral waters. *Journal of Maps* **12** (5), 917–935.

Deutsch, W. J. 1997 *Groundwater Geochemistry, Fundamentals and Applications to Contamination.* Lewis, New York, USA.

Dubrovsky, N. M., Deverel, S. J. & Gilliom, R. J. 1993 Multiscale approach to regional ground water quality assessment: selenium in the San Joaquin Valley, California. In: *Regional Ground Water Quality* (W. M. Alley, ed.), Van Nostrand Reinhold, New York, USA, pp. 537–562.

Edmunds, W. M. 2009 Geochemistry's vital contribution to solving water resource problems. *Appl. Geochem.* **24**, 1058–1073.

Fidelibus, M. D. & Tulipano, L. 1996 Regional flow of intruding sea water in the carbonate aquifers of Apulia (Southern

Italy). In: *Proceedings 14th Salt Water Intrusion Meeting, Rapporter och meddelanden nr 87*, pp. 230–241.

Fujii, R. F. & Swain, W. C. 1995 *Areal Distribution of Selected Trace Elements, Salinity, and Major Ions in Shallow Ground Water, Tulare Basin, Southern San Joaquin Valley, California*. US Geol. Surv. Water-Resour. Invest. Rep. 95-4048, US Geological Survey, Sacramento, CA, USA.

Kortatsi, B. K., Tay, C. K., Anornu, G., Hayford, E. & Dartey, G. A. 2008 Hydrogeochemical evaluation of groundwater in the lower Offin basin, Ghana. *Environmental Geology* **53** (8), 1651–1662.

Machiwal, D. & Jha, M. K. 2015 Identifying sources of groundwater contamination in a hard-rock aquifer system using multivariate statistical analyses and GIS-based geostatistical modeling techniques. *J. Hydrol. Reg. Stud.* **4**, 80–110.

Mayo, A. L. & Loucks, M. D. 1995 Solute and isotopic geochemistry and groundwater flow in the Central Wasatch Range, Utah. *J. Hydrol.* **172**, 31–59.

Nordstrom, D. K., Ball, J. W., Donahoe, R. J. & Whittemore, D. 1989 Groundwater chemistry and water-rock interactions at Stripa. *Geochim. Cosmochim. Acta* **53**, 1727–1740.

Satyanarayanan, M., Eswaramoorthi, S., Subramanian, S. & Periakali, P. 2016 Factor analysis of rock, soil and water geochemical data from Salem magnesite mines and surrounding area, Salem, southern India. *Appl. Water. Sci* **7**, 2607–2616.

Schoeller, H. 1962 *Les Eaux Souterraines*. Masson et Cie, Editeurs, Paris, France.

Seiler, R. L., Skorupa, J. P., Naftz, D. L. & Nolan, B. T. 2003 *Irrigation-Induced Contamination of Water, Sediment, and Biota in the Western United States: Synthesis of Data from the National Irrigation Water Quality Program*. US Geol. Surv. Prof. Paper 1655, US Geological Survey, Denver, CO, USA.

Sinani, V., Sana, M., Seferi, E. & Sinani, A. 2014 The impact of natural water quality on baking products in Albania. *Journal of Water Resource and Protection* **6**, 1659–1665.

Szabo, Z., Rice, D. E., McLeod, C. L. & Barringer, T. H. 1997 *Relation of Distribution of Radium, Nitrate, and Pesticides to Agricultural Land Use and Depth, Kirkwood–Cohansey Aquifer System, New Jersey Coastal Plain, 1990–91*. US Geol. Surv. Water – Resour. Invest. Rep. 96-4165A, US Geological Survey, Denver, CO, USA.

Vidal Montes, R., Martinez-Graña, A. M., Martínez Catalán, J. R., Ayarza Arribas, P. & Sánchez San Román, F. J. 2016 Vulnerability to groundwater contamination, SW salamanca, Spain. *Journal of Maps*, **12** (suppl.), 147–155.

First received 4 March 2017; accepted in revised form 20 April 2017. Available online 23 May 2017